Femtosecond broadband fluorescence upconversion spectroscopy: Spectral coverage versus efficiency

Gerecke, Mario; Bierhance, Genaro; Gutmann, Michael; Ernsting, Nikolaus P.; Rosspeintner, Arnulf

Femtosecond broadband fluorescence upconversion spectroscopy: Spectral coverage versus efficiency

Mario Gerecke,[1] Genaro Bierhance,[1] Michael Gutmann,[2] Nikolaus P. Ernsting,[1,a)] and Arnulf Rosspeintner[3,a)]
[1]*Department of Chemistry, Humboldt-Universität zu Berlin, Brook-Taylor-St. 2, D-12489 Berlin, Germany*
[2]*LIOP-TEC GmbH, Industriestrasse 4, D-42477 Radevormwald, Germany*
[3]*Département de Chimie Physique, Université de Genève, 30, Quai Ernest-Ansermet, 1211 Genève 4, Switzerland*

(Received 3 February 2016; accepted 22 April 2016; published online 16 May 2016)

Sum frequency mixing of fluorescence and ~1300 nm gate pulses, in a thin β-barium borate crystal and non-collinear type II geometry, is quantified as part of a femtosecond fluorimeter [X.-X. Zhang *et al.*, Rev. Sci. Instrum. **82**, 063108 (2011)]. For a series of fixed phasematching angles, the upconversion efficiency is measured depending on fluorescence wavelength. Two useful orientations of the crystal are related by rotation around the surface normal. Orientation A has higher efficiency (factor ~3) compared to B at the cost of some loss of spectral coverage for a given crystal angle. It should be used when subtle changes of an otherwise stationary emission band are to be monitored. With orientation B, the fluorescence range λ_F > 420-750 nm is covered with a single setting of the crystal and less gate scatter around time zero. The accuracy of determining an instantaneous emission band shape is demonstrated by comparing results from two laboratories. *Published by AIP Publishing.* [http://dx.doi.org/10.1063/1.4948932]

INTRODUCTION

To watch fluorescence with <100 fs time resolution and flat spectral response has been a dream of photochemists and physicists for decades. Careful measurement of the spectral evolution allows us to establish (or reject) models for chromophore-environment coupling and the relevant dynamical variables. The more accurate and precise the observation of an instantaneous emission spectrum, the more forceful will be conclusions about the underlying couplings and processes.[1–3] In general, if transient fluorescence band shapes are to be used in a quantitative way, then their photometric accuracy must be ensured. As a corollary, transient spectra of the same sample, but from different laboratories, should be identical. Here we test that principle for broadband fluorescence upconversion spectroscopy (FLUPS).[4–7]

Fluorescence gating has been performed with a Kerr shutter,[8–15] by non-collinear optical parametric amplification[16–20] or by diffraction from a transient grating,[21] in addition to broadband upconversion schemes.[4–7,22–25] Here we consider only reports where spontaneous emission from molecular or similar sources is gated, dispersed, and registered simultaneously at all relevant wavelengths with a view to obtain true molecular spectra. Principal problems relate to the spectral bandwidth, the contrast (i.e., the number of gated photons from the sample relative to others), and to the time resolution.

Non-collinear parametric fluorescence amplification looks attractive as extremely high signal levels can be achieved, well visible to the eye.[18,19] However, gain narrowing may deform the spectrum of the seed and superfluorescence background is always present, in principle, to the same order of magnitude as the signal. Both aspects fluctuate strongly with the gating pump power and mode structure. As a consequence, the photometric characterization of fluorescence amplification turned out to be unstable in our experiments.

The Kerr shutter is the most established gating device for broadband fluorescence probably because phasematching need not be considered. In initial work, a difficulty was presented by the limited extinction ratio of a polarizing wire grid,[10,11] but this drawback has since been removed by the use of a thin Glan polarizer.[12,13] Only the achievable width Δt of the instrumental response function is larger compared to other methods, when the optimal Kerr medium (benzene) is used.

In this paper, we examine sum frequency mixing of λ_F = 420-750 nm fluorescence light with λ_G = ~1340 nm gate pulses in a thin β-barium borate (BBO) crystal to result in upconverted light at λ_U. The setup in Fig. 1 improves over the one in Ref. 6 in terms of efficiency and bandwidth in addition to better handling in practice. The essential difference is the introduction of calcite prism C[7] and the use of a BBO crystal. A complete description of the device and procedures is provided in the supplementary material.[30]

The prism is cut with the calcite optical axis orthogonal to the refracting edge and in the input plane. Thus the vertically polarized fluorescence is deviated more than the horizontally polarized one, and the latter can be removed with a beam stop. In addition, the prism causes angular dispersion (~1.3° between 420 and 750 nm) which aids in phase-matching (see below). The prism edge just intercepts an intermediate fluorescence waist so that the amount of material traversed is minimal.

The vertically polarized fluorescence is then focussed onto the BBO crystal from the left. Here it interacts with

a)Authors to whom correspondence should be addressed. Electronic addresses: nernst@chemie.hu-berlin.de, Arnulf.Rosspeintner@unige.ch

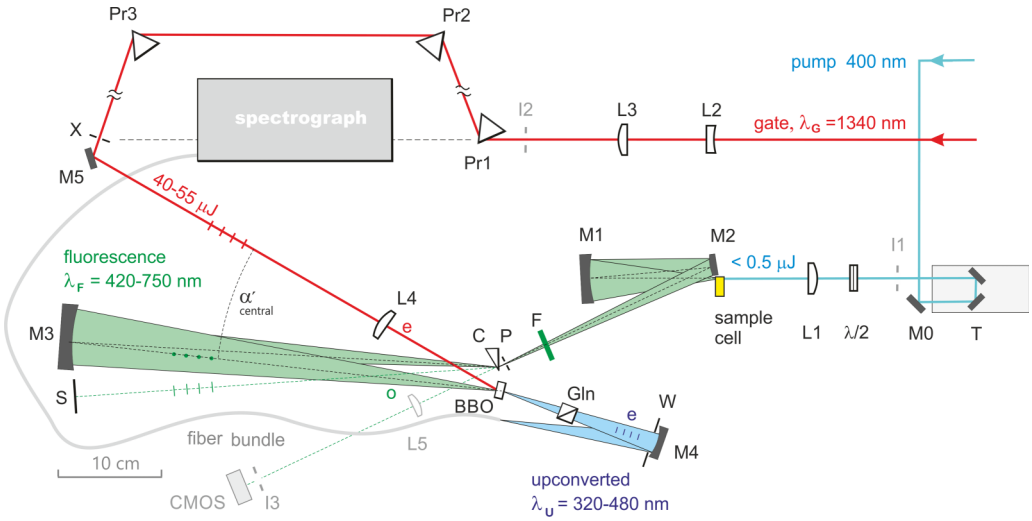

FIG. 1. Generic setup for broadband fluorescence upconversion. M—mirrors, Pr—prisms, L—lenses, F—long-pass ($\lambda_F \geq 420$ nm) dielectric filter, P—800 μm pinhole for alignment, C—calcite prism, Gln—optional Glan polarizer, W—tunable window, S—stop for horizontally polarized fluorescence, X—~3 mm iris. See the supplementary material[30] for specifications and differences between the arrangements in Geneva and Berlin. The introduction of C, to both polarize and partly disperse the fluorescence, and the use of a BBO crystal represent the essential differences to Ref. 6. (Note that Kerr gating can be performed with this setup also, after small modifications, since crossed C and Gln have $<10^{-5}$ extinction ratio.)

gate pulses, which are polarized horizontally and also enter from the left. The optical axis of the BBO crystal is located in the horizontal plane so that fluorescence forms an ordinary (o) and the gate an extraordinary (e) beam for type II sum-frequency generation. The upconverted signal is horizontally polarized, corresponding to an extraordinary (e) beam. A large interaction angle between fluorescence and gate, $\alpha'_{\text{central}} = 20°\text{-}25°$, is advantageous both for phasematching and for background-free detection of the upconverted signal (see Fig. 2).

The actual crystal setting is specified by the input angle $\delta'_{\text{F central}}$ for the central fluorescence ray. Note that α'_{central} is given by the beam geometry and remains unaltered when the BBO crystal is tuned.

The backbone of this work consists in precision measurements of the upconversion efficiency as a function of detection wavelength λ_U. The procedure is as follows. A stationary reference spectrometer provides fluorescence quantum distributions $f_i^{(F)}(\lambda_F)$ for standard dye solutions i. These are transformed *in silico* to the expected distributions $f_i^{(U)}(\lambda_U)$ of upconverted photons. We also measure the raw signal spectra $s_i^{(U)}(\lambda_U)$ for a late delay time when all relaxation processes have ceased. Division of expected and measured spectra gives a number of overlapping correction functions $CF_i(\lambda_U) = f_i^{(U)}(\lambda_U)/s_i^{(U)}(\lambda_U)$ which, together, cover the range $\lambda_U = 320\text{-}480$ nm. By comparison of noise in the overlap regions, a unique contiguous correction function $CF(\lambda_U)$ is obtained.[26] For its application, consider the spectral evolution of a sample x to be investigated. Multiplication of every recorded upconverted spectrum $s_x^{(U)}(t, \lambda_U)$ with $CF(\lambda_U)$ gives $f_x^{(U)}(t, \lambda_U)$, i.e., a copy of the true molecular fluorescence evolution in the ultraviolet range.

The focus of this work is on how the correction function CF depends on the input angle $\delta'_{\text{F central}}$ and the orientation of the BBO crystal, which are the key parameters for successful FLUPS measurements.

EXPERIMENTAL SECTION

The interaction region is zoomed up in Fig. 2, where the paper plane represents the optical table. The BBO crystal (from Eksma Optics) has cut angle $\theta_N = 40°$ ($\varphi_N = 0°$) and is 100 μm thick. Two crystal-fixed Cartesian coordinate systems are used. The one for the input surface is shown on the left.

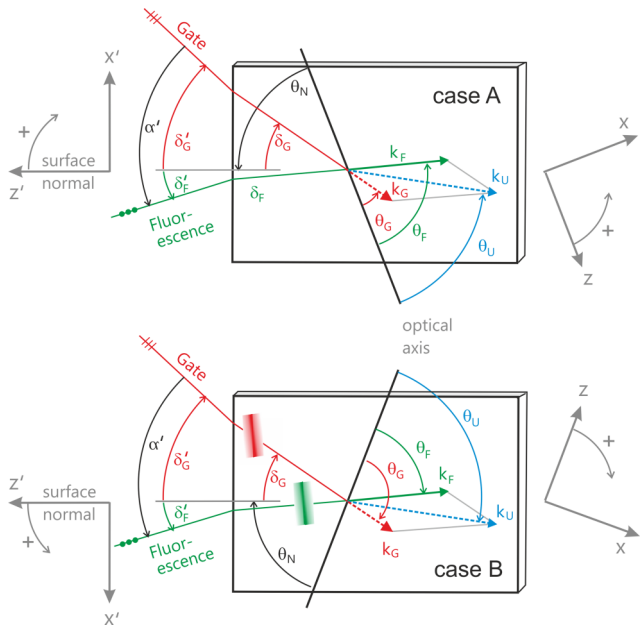

FIG. 2. View of the interaction geometry from the top with crystal-fixed coordinate systems. Optical input is from the left and output towards the right. A large angle $\alpha' \approx 20°\text{-}25°$ between the gate ($\lambda_G = 1340$ nm) and fluorescence beam helps to provide broad spectral coverage for a fixed setting of the β-barium borate crystal. Two cases are distinguished by the order in which wave vectors $\vec{k}_G$, $\vec{k}_F$ form internal angles with the optical axis (dashed wave vector—extraordinary polarization, solid—ordinary). Intensity cross correlation width <100 fs (fwhm) can be achieved by tilting of the gate pulse front, as indicated in the lower part.

Here $\vec{z}'$ is the surface normal, and $\vec{x}'$ is the horizontal axis in the crystal surface to which the optical axis comes closer. In this direction from $\vec{x}'$, we have positive external input angles δ'. The internal coordinate system $(\vec{z}, \vec{x})$ is shown on the right. Now $\vec{z}$ is the optical axis of the crystal considered positive in the direction of the output normal. $\vec{x}$ is that orthogonal unit vector in the table plane which has a positive component with $\vec{k}_U$. Generally, external angles are written primed and internal angles unprimed.

Two orientations of the crystal, or cases, are distinguished by the order in which wavevectors $\vec{k}_G$ and $\vec{k}_F$ form internal angles with the optical axis. They are related by a 180° rotation around the surface normal and found experimentally by minimizing doubled gate light. In case A, $\vec{k}_G$ is closer and $\vec{k}_F$ is further away from the optical axis. For example, this can be achieved with $\delta'_F = -3°$ and $\delta'_G = +18°$ as shown qualitatively in the upper part of the figure. In case B, instead, $\vec{k}_F$ is closer to the optical axis compared to $\vec{k}_G$ as shown in the lower part of Fig. 2. Now, for example, $\delta'_F = +3°$ and $\delta'_G = -18°$. (Note that in the main text, we refer to a setup in Geneva which has $\alpha'_{central} = 21°$. In the supplementary material, the equivalent material is presented for a setup in Berlin, where $\alpha'_{central} = 23°$.)[30]

Dye solutions are prepared in 1 mm cuvettes of fused silica, namely, BBOT, C6H, C153, and DCM (see supplementary material[30]) in acetonitrile. For replacement of sample in the excited volume, it is sufficient to bubble a faint stream of N_2 through the cell. The pump-probe delay is advanced to 250 ps for calibration measurements. By this late time spectral shifts and changes of shape have ceased for these molecular systems. Also spectral relaxation in acetonitrile is fast enough, compared to the fluorescence lifetime, so that the spectrum at 250 ps may be equated with the stationary one.

In experiments, first the desired crystal orientation is chosen. In a series of subsequent measurements, we set the angle $\delta'_{F\,central}$ between surface normal and incoming fluorescence light cone (using the central ray or the unblocked pump) with the help of a calibrated rotation table. All other angles are now determined. With this arrangement, the "technical" signal- or count-distribution in the UV over pixels p, i.e., the raw upconverted spectrum $s^{(U)}(p)$, is recorded for the four dye solutions. The resulting set of partial correction functions is then merged into a contiguous photometric correction function $CF(p)$.[26] The entire procedure is fast enough so that it can be performed on a daily basis. Note that the linear spectrograph calibration $p(\lambda_U)$ in the UV allows us to write the correction function as $CF(\lambda_U)$.

RESULTS AND DISCUSSION

Experimental results are shown in the left panels of Fig. 3. They contain the measured (multiplicative) correction functions $CF(\lambda_U)$ for several crystal angles. The corresponding fluorescence wavelengths λ_F are marked on the upper border of the figure. For example, consider that a large time-dependent Stokes shift (TDSS) is to be followed after excitation at 400 nm.[3] For this purpose, one would chose case B with $\delta'_{F\,central} = 3.5°$, which can be set reproducibly with the calibrated rotation table on which the crystal is mounted. With this setting, a transient fluorescence spectrum in the range 420-750 nm requires less correction (amplitude factor <3) than with a normal stationary fluorimeter. Alternatively one might want to follow

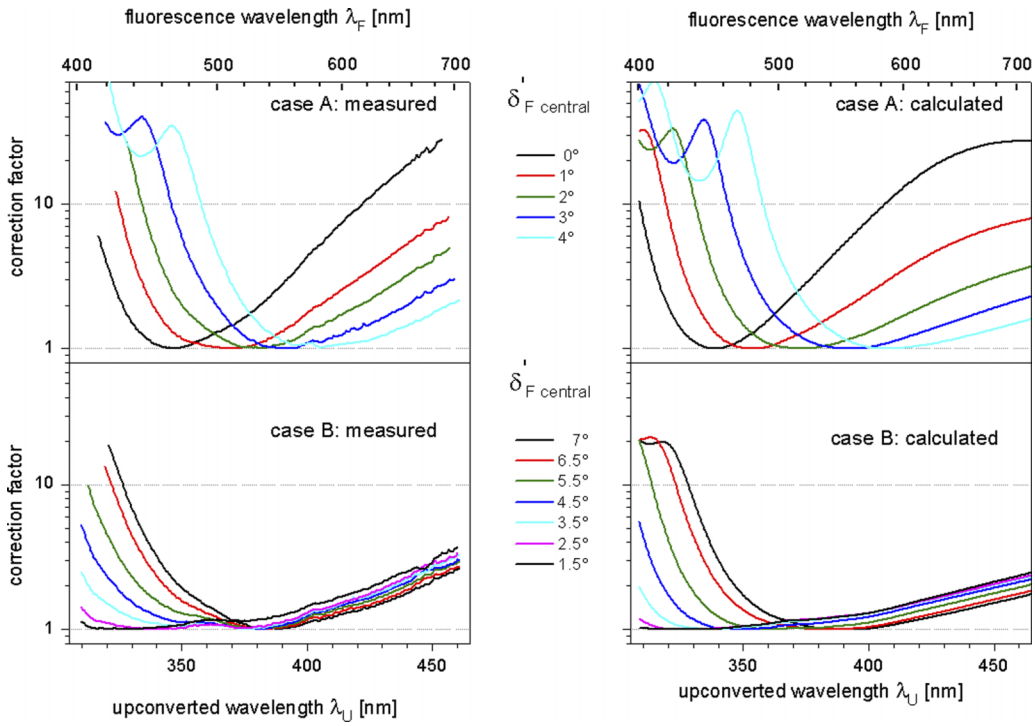

FIG. 3. Measured (left) and calculated (right) correction factors over upconverted wavelengths λ_U for the FLUPS setup having $\alpha'_{central} = 21°$. The BBO crystal has cut angle $\theta_N = 40°$ ($\varphi_N = 0°$) and is 100 μm thick. Curves have been normalized at the minimum.

the disappearance of a vibrational shoulder in the emission spectrum of a cyanine dye.[27] Now small spectral changes must be monitored in the fluorescence range 530-670 nm, which is best achieved with case A (which has better peak efficiency) at $\delta'_{\mathrm{F\ central}} = -4.0°$.

Corresponding calculation results are shown in the right panels of Fig. 3. We start with the quantum efficiency of upconversion $F \rightarrow U$. For small-power transfer, one has[28]

$$\eta_{\mathrm{total}} = \frac{N_{\mathrm{U}}(z=L)}{N_{\mathrm{F}}(z=0)} \propto I_{\mathrm{G}}(z=0)\left\{\frac{\omega_{\mathrm{U}}\omega_{\mathrm{F}}d_{\mathrm{eff}}^2}{n_{\mathrm{e}}(\omega_{\mathrm{U}})\,n_{\mathrm{o}}(\omega_{\mathrm{F}})\,n_{\mathrm{e}}(\omega_{\mathrm{G}})}\right\} \times\left[\frac{\sin(\Delta kL/2)}{\Delta kL/2}\right]^2 L^2. \quad (1)$$

Here N_{F} is the photon flux, I_{G} the gate intensity, ω_x an angular frequency, n_x an index of refraction, d_{eff} the effective nonlinearity, Δk the phase mismatch, and L the crystal thickness. Because G and U are extraordinarily polarized, the refractive index n_{e} of the BBO medium for these waves depends on the angle θ between the corresponding wave vector and the optical axis (see Fig. 2). In addition to this intrinsic flux ratio, technical efficiency factors T must be applied to the upconverted photon flux N_{U} to account for spectrograph transmission and CCD quantum efficiency. The algorithms for calculating η_{total} and all relevant data are given in the supplementary material.[30] Since a range of fluorescence angles $\Delta\delta'_{\mathrm{F}} = \pm 2.5°$ around $\delta'_{\mathrm{F\ central}}$ is collected (see Fig. 1), we average η_{total} correspondingly. The correction function is then estimated to be $\sim(T\,\eta_{\mathrm{total}})^{-1}$. The calculated $CF\,(\lambda_{\mathrm{U}})$ curves reflect the relative size, order, and shape of the measured curves extremely well.

The gate pulses are always frequency-doubled, due to their high intensity, to form a red beam behind the non-linear optical (NLO) crystal. Cases A or B correspond to minimum SHG as the crystal is rotated around the surface normal, but the two minima are visually different from each other. In case A, the minimum red intensity is higher and the intensity rises, upon rotation around the normal, steeper compared to case B (for details see the supplementary material).[30] Upconverted scatter from the input surface appears at $\lambda_{\mathrm{U}} \approx 440$ nm and may corrupt the upconverted fluorescence signal there around time zero. Case B should be chosen to minimize this problem.

We conclude that our upconversion spectrometer is understood quantitatively. It allows the determination of truly molecular fluorescence band shapes with <100 fs time resolution at a single fixed setting of the NLO crystal. To prove this point, we measured the fluorescence band of Coumarin 153 in dimethyl-sulfoxide in two separate setups. Instantaneous emission spectra at 1 ps and 500 ps are compared in Fig. 4. For example, at 1 ps, the peak wavenumber is 19 270 (19 380) cm^{-1}, the width parameter Δ is 3520 (3680) cm^{-1}, and the asymmetry parameter γ is −0.29 (−0.34) (from a lognorm fit, see supplementary material[30]). Even though the experimental conditions were different, the time-resolved molecular emission spectra are practically identical, considering the standards of fluorescence spectrophotometry.[26]

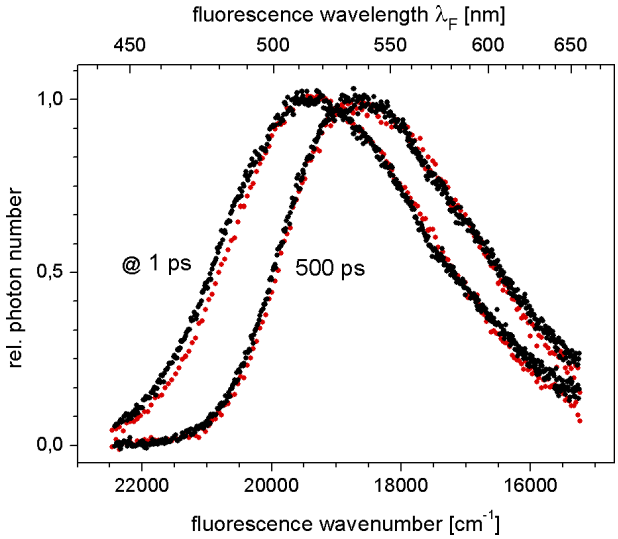

FIG. 4. Instantaneous emission of Coumarin 153 in dimethyl-sulfoxide measured and corrected in Berlin (*black dots*, $\alpha'_{\mathrm{central}} = 23°$ for the central ray) and Geneva (*red*, $\alpha'_{\mathrm{central}} = 21°$) using case B. Shown are photon distributions over fluorescence wavenumber normalized at the peak (see supplementary material[30]).

OUTLOOK

Perspectives for improvement open up when the useful input angles δ'_{F} for a given fluorescence wavelength λ_{F} are considered. In Fig. 5, we show curves $\delta'_{\mathrm{F}}(\lambda_{\mathrm{F}})$ for exact phasematching $\Delta k = 0$ as solid black lines. They are surrounded by regions of tolerance phasematching, $0 < |\Delta k| < \pi/L$. All curves were calculated with the assumption that the crystal is tuned to exact phasematching at $\lambda_{\mathrm{F}} = 500$ nm and fixed there, corresponding to $\delta'_{\mathrm{F\ central}} = +1.5°$ (horizontal dashed line in A) or +2.6° (B). The topology of the tolerance region is characteristically different for the two cases (for an explanation, the reader is referred to the supplementary material[30]). The cone of fluorescence which is focused onto the crystal is represented by a green shaded band (±2.5°) around $\delta'_{\mathrm{F\ central}}$. Here the two spatial aspects are discussed in search of higher upconversion efficiency.

In case A (*upper panel*) the angles δ'_{F} and α' which satisfy the exact phasematching condition strongly depend on fluorescence wavelength. For example, the slope of the solid black line (where $\Delta k = 0$) at the cross of dashed lines is about 5° over 40 nm. If $\Delta k = 0$ were strictly necessary, then a fluorescence slice of only 40 nm would be observed. But instead, our results show an efficient range $\lambda_{\mathrm{F}} = 440$-730 nm ($CF \leq 10$, say, for $\delta'_{\mathrm{F\ central}} = 1.5°$ in Fig. 3 top left). The upconverted signal is therefore mostly generated with tolerance-phasematching. Returning to Fig. 5(a), we see that for all $\lambda_{\mathrm{F}} > 440$ nm, the full fluorescence cone falls into the tolerance region. It follows that the full cone is brought into the upconversion process in case A (an observation which is readily checked by obscuring parts of mirror M_3). This improves sensitivity in addition to the already higher intrinsic efficiency compared to case B.[30]

In case B (*lower panel*), the situation is reversed. The values for δ'_{F} at the limits for our observation range ($\lambda_{\mathrm{F}} = 420$ and 750 nm) differ by less than 2.5°. However for each λ_{F},

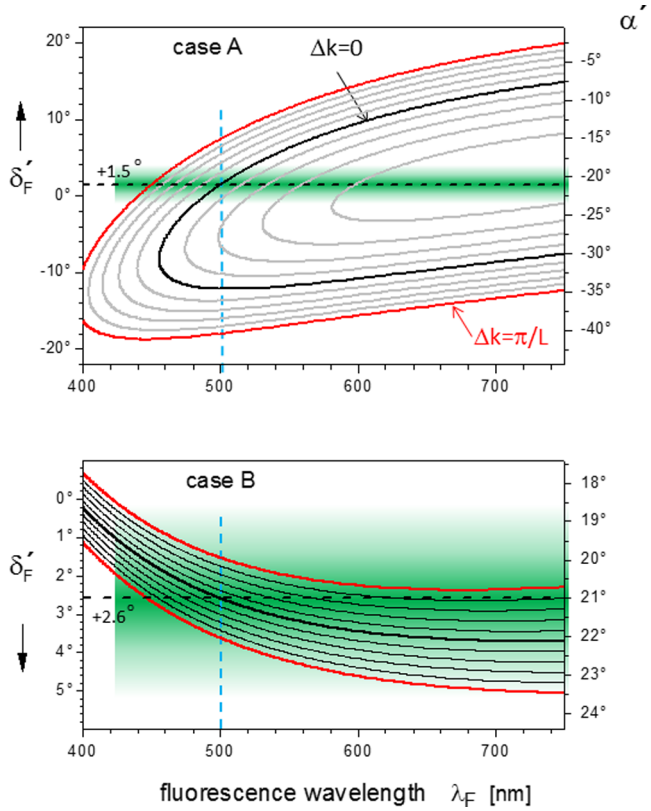

FIG. 5. External fluorescence angle δ_F' depending on wavelength λ_F. In this example, the crystal is set to perfect phasematching $\Delta k = 0$ at 500 nm for the central ray, which has $|\alpha'_{\text{central}}| = 21°$ by construction of the setup (dashed lines). A range of angles, indicated by the green shaded area, contributes to upconversion. Note the different vertical scales; their direction reflects the absolute layout on the table. In case A, the dispersion for perfect phasematching is relatively strong, but tolerance-phasematching $0 < |\Delta k| < \pi/L$ is possible in a large angular range. In case B, the situation is reversed.

the angular range for tolerance covers only part of the full fluorescence cone. The crystal accepts only narrow strips of fluorescence, which are spread across the refocussing mirror M_3 according to λ_F. We conclude from this observation that angular dispersion with the help of prism C may improve the efficiency. In the arrangement of Fig. 1, the dispersion due to C, which currently is relatively small, has a direction which is consistent with the phasematching requirement. Its range and shape should be optimized for achromatic phasematching.[29]

ACKNOWLEDGMENTS

We thank the Deutsche Forschungsgemeinschaft (Grant to N.P.E. in Collaborative Research Area 1078 "Protonation Dynamics in Protein Function"), the Fonds National Suisse de la Recherche Scientifique (Project No. 200020-147098), and the University of Geneva for financial support. A.R. thanks Eric Vauthey and Bernhard Lang for continued support.

[1]O. Braem, T. J. Penfold, A. Cannizzo, and M. Chergui, Phys. Chem. Chem. Phys. **14**, 3513 (2012).
[2]Y. Kimura, M. Fukuda, K. Suda, and M. Terazima, J. Phys. Chem. B **114**, 11847 (2010).
[3]M. Sajadi, F. Berndt, C. Richter, M. Gerecke, R. Mahrwald, and N. P. Ernsting, J. Phys. Chem. Lett. **5**, 1845 (2014).
[4]R. Schanz, S. A. Kovalenko, V. Kharlanov, and N. P. Ernsting, Appl. Phys. Lett. **79**, 566 (2001).
[5]L. Zhao, L. P. Lustres, V. Farztdinov, and N. P. Ernsting, Phys. Chem. Chem. Phys. **7**, 1716 (2005).
[6]X.-X. Zhang, C. Würth, L. Zhao, U. Resch-Genger, N. P. Ernsting, and M. Sajadi, Rev. Sci. Instrum. **82**, 063108 (2011).
[7]M. Sajadi, M. Quick, and N. P. Ernsting, Appl. Phys. Lett. **103**, 173514 (2013).
[8]S. Kinoshita, H. Ozawa, Y. Kanematsu, I. Tanaka, N. Sugimoto, and S. Fujiwara, Rev. Sci. Instrum. **71**, 3317 (2000).
[9]J. Takeda, K. Nakajima, S. Kurita, S. Tomimoto, S. Saito, and T. Suemoto, Phys. Rev. B **62**, 10083 (2000).
[10]B. Schmidt, S. Laimgruber, W. Zinth, and P. Gilch, Appl. Phys. B **76**, 809 (2003).
[11]S. Arzhantsev and M. Maroncelli, Appl. Spectrosc. **59**, 206 (2005).
[12]N. P. Ernsting, J. Breffke, D. Y. Vorobyev, D. A. Duncan, and I. Pfeffer, Phys. Chem. Chem. Phys. **10**, 2043 (2008).
[13]M. Sajadi, A. L. Dobryakov, E. Garbin, N. P. Ernsting, and S. A. Kovalenko, Chem. Phys. Lett. **489**, 44 (2010).
[14]T. Fujiwara, N. C. Romano, and E. C. Lim, Opt. Commun. **315**, 324 (2014).
[15]K. Appavoo and M. Y. Sfeir, Rev. Sci. Instrum. **85**, 055114 (2014).
[16]P. Fita, Y. Stepanenko, and C. Radzewicz, Appl. Phys. Lett. **86**, 021909 (2005).
[17]H. Chen, Y. Weng, and J. Zhang, J. Opt. Soc. Am. B **26**, 1627 (2009).
[18]S. Du, D. Zhang, Y. Shi, Q. Li, B. Feng, X. Han, Y. Wenig, and J.-Y. Zhang, Opt. Commun. **282**, 1884 (2009).
[19]Q. Ding, K. Meng, H. Yang, S. Wang, and Q. Gong, Opt. Commun. **284**, 3110 (2011).
[20]W. Dang, P. Mao, and Y. Weng, Rev. Sci. Instrum. **84**, 073105 (2013).
[21]K. Chen, J. K. Gallaher, A. J. Barker, and J. M. Hodgkiss, J. Phys. Chem. Lett. **5**, 1732 (2014).
[22]G. Zgrablić, K. Voïtchovsky, M. Kindermann, S. Haacke, and M. Chergui, Biophys. J. **88**, 2779 (2005).
[23]A. Cannizzo, O. Bräm, G. Zgrablić, A. Tortschanoff, A. Ajdarzadeh Oskouei, F. van Mourik, and M. Chergui, Opt. Lett. **32**, 3555 (2007).
[24]J. Léonard, T. Gelot, K. Torgasin, and S. Haacke, J. Phys.: Conf. Ser. **277**, 012017 (2011).
[25]J. Sung, P. Kim, B. Fimmel, F. Würthner, and D. Kim, Nat. Commun. **6**, 8646 (2015).
[26]J. A. Gardecki and M. Maroncelli, Appl. Spectrosc. **52**, 1179 (1998).
[27]V. Karunakaran, L. P. Lustres, L. Zhao, N. P. Ernsting, and O. Seitz, J. Am. Chem. Soc. **128**, 2954 (2006).
[28]F. Zernicke and J. E. Midwinter, *Applied Nonlinear Optics* (Wiley, New York, 1973).
[29]O. E. Martinez, IEEE J. Quantum Electron. **25**, 2464 (1989).
[30]See supplementary material at http://dx.doi.org/10.1063/1.4948932 for a detailed description of the experimental setup, the theoretical calculation, and experimental measurement of the photometric correction function, details on the phase-matching conditions for FLUPS and the collinear SHG by the gate pulses.